Inorg. Chem. **2005**, *44*, 6482–6492

Highly Cross-linked Polymers Containing *N*,*N*′,*N*′′-Chelate Ligands for the Cu(II)-Mediated Hydrolysis of Phosphoesters

Alexander Schiller, Rosario Scopelliti, Meriem Benmelouka, and Kay Severin*

Institut des Sciences et Ingénieries Chimiques, École Polytechnique Fédérale de Lausanne (EPFL), 1015 Lausanne, Switzerland

Received March 28, 2005

Three immobilized Cu(II) complexes were generated by the following: (a) homopolymerization of the *N*,*N*′,*N*′′-chelate ligand tris[2-(1-vinylimidazolyl)]phosphine (**1**) and subsequent metalation with $CuCl_2$; (b) copolymerization of **1** with ethyleneglycol dimethacrylate (EGDMA) und subsequent metalation with $CuCl_2$; or (c) molecular imprinting with the organometallic Mo-complex [Mo(η^3-C_4H_7)$(CO)_2$(**1**)](TsO) (**5**) and EGDMA and subsequent replacement of Mo(II) by Cu(II). All three polymeric Cu complexes were found to efficiently promote the hydrolysis of activated phosphoesters with the relative activity being dependent on the nature of the polymer and the substrate.

Introduction

Copper(II) complexes of bi- and tridentate N-donor ligands such as bipyridine,[1] terpyridine,[2] and 1,4,7-triazacyclononane[3] and their derivatives have been investigated intensively as artificial phosphoesterases.[4] Being substitutionally labile and a strong Lewis acid, Cu^{2+} is well-suited for such reactions. Compared to structurally related complexes of other M^{2+} ions such as Zn^{2+}, copper complexes often show a superior performance.[4] Nevertheless, most Cu-based synthetic phosphoesterases described so far display some drawbacks. A general problem, which is shared by many other biomimetic hydrolases, was found to be product inhibition, resulting in low catalytic turnover.[4] Another setback frequently encountered was the formation of catalytically inactive hydroxy-bridged dimers $[L_nCu(\mu\text{-}OH)_2CuL_n]^{2+}$ (L_n = multidentate N-donor ligand).[1c,e,2b,c,g,3a,c,d,f] To circumvent this unfavorable dimer formation, sterically demanding groups were attached to the N-donor ligands. This strategy has been quite successful in producing complexes with an enhanced catalytic activity but an obvious drawback of such an approach is the reduced accessibility of the metal center. Furthermore, these groups may lead to a lower solubility of the catalyst in aqueous solution. The immobilization of Cu complexes on solid supports offers a potential alternative to reduce problems of aggregation and solubility and our efforts in this direction are reported below.

A number of immobilized copper complexes with esterase activity were recently reported. The respective ligand was either covalently attached to a silica surface,[5] or to polysty-

* E-mail: kay.severin@epfl.ch.

(1) (a) Liu, S.; Hamilton, A. D. *Chem. Commun.* **1999**, 587−588. (b) Kövári, E.; Krämer, R. *J. Am. Chem. Soc.* **1996**, *118*, 12704−12709. (c) Linkletter, B.; Chin, J. *Angew. Chem., Int. Ed. Engl.* **1995**, *34*, 472−474. (d) Morrow, J. R.; Trogler, W. C. *Inorg. Chem.* **1989**, *28*, 2330−2333. (e) Morrow, J. R.; Trogler, W. C. *Inorg. Chem.* **1988**, *27*, 3387−3394.

(2) (a) Sakamoto, S.; Tamura, T.; Furukawa, T.; Komatsu, Y.; Ohtsuka, E.; Kitamura, M.; Inoue, H. *Nucl. Acids Res.* **2003**, *31*, 1416−1425. (b) Putnam, W. C.; Daniher, A. T.; Trawick, B. N.; Bashkin, J. K. *Nucl. Acids Res.* **2001**, *29*, 2199−2204. (c) Jenkins, L. A.; Bashkin, J. K.; Pennock, J. D.; Florián, J.; Warshel, A. *Inorg. Chem.* **1999**, *38*, 3215−3222. (d) Jurek, P. E.; Martell, A. E. *Inorg. Chem.* **1999**, *38*, 6003−6007. (e) Inoue, H.; Furukawa, T.; Shimizu, M.; Tamura, T.; Matsui, M.; Ohtsuka, E. *Chem. Commun.* **1999**, 45−46. (f) Daniher, A. T.; Bashkin, J. K. *Chem. Commun.* **1998**, 1077−1078. (g) Liu, S.; Hamilton, A. D. *Tetrahedron Lett.* **1997**, *38*, 1107−1110. (h) Suh, J.; Lee, J. Y.; Hong, S. H. *Bioorg. Med. Chem. Lett.* **1997**, *7*, 2383−2386. (i) Bashkin, J. K.; Frolova, E. I.; Sampath, U. *J. Am. Chem. Soc.* **1994**, *116*, 5981−5982. (j) Bashkin, J. K.; Jenkins, L. A. *J. Chem. Soc., Dalton Trans.* **1993**, 3631−3632. (k) Stern, M. K.; Bashkin, J. K.; Sall, E. D. *J. Am. Chem. Soc.* **1990**, *112*, 5357−5359.

(3) (a) Fry, F. H.; Fischmann, A. J.; Belousoff, M. J.; Spiccia, L.; Brügger, J. *Inorg. Chem.* **2005**, *44*, 941−950. (b) Iranzo, O.; Richard, J. P.; Morrow, J. R. *Inorg. Chem.* **2004**, *43*, 1743−1750. (c) Fry, F. H.; Spiccia, L.; Jensen, P.; Moubaraki, B.; Murray, K. S.; Tiekink, E. R. T. *Inorg. Chem.* **2003**, *42*, 5594−5603. (d) Deck, K. M.; Tseng, T. A.; Burstyn, J. N. *Inorg. Chem.* **2002**, *41*, 669−677. (e) McCue, K. P.; Morrow, J. R. *Inorg. Chem.* **1999**, *38*, 6136−6142. (f) Hegg, E. L.; Mortimore, S. H.; Cheung, C. L.; Huyett, J. E.; Powell, D. R.; Burstyn, J. N. *Inorg. Chem.* **1999**, *38*, 2961−2968. (g) McCue, K. P.; Voss, D. A. J.; Marks, C.; Morrow, J. R. *J. Chem. Soc., Dalton Trans.* **1998**, 2961−2963. (h) Hegg, E. L.; Deal, K. A.; Kiessling, L. L.; Burstyn, J. N. *Inorg. Chem.* **1997**, *36*, 1715−1718. (i) Hegg, E. L.; Burstyn, J. N. *Inorg. Chem.* **1996**, *35*, 7474−7481. (j) Young, M. J.; Chin, J. *J. Am. Chem. Soc.* **1995**, *117*, 10577−10578.

(4) For reviews see: (a) Molenveld, P.; Engbersen, J. F. J.; Reinhoudt, D. N. *Chem. Soc. Rev.* **2000**, *29*, 75−86. (b) Krämer, R. *Coord. Chem. Rev.* **1999**, *182*, 243−261. (c) Bashkin, J. K. *Curr. Opin. Chem. Biol.* **1999**, *3*, 752−758. (d) Hegg, E. L.; Burstyn, J. N. *Coord. Chem. Rev.* **1998**, *173*, 133−165. (e) Chin, J. *Curr. Opin. Chem. Biol.* **1997**, *1*, 514−521.

10.1021/ic0504588 CCC: $30.25
Published on Web 08/12/2005

Scheme 1. Synthesis of Three Different Coordinating Polymers by (a) Homopolymerization of the Chelate Ligand **1** To Give **P1**, (b) Copolymerization of **1** with EGDMA To Give **P2,** or (c) Copolymerization of a Metal Complex (**1**)ML_n and Subsequent Cleavage of the Metal Fragment ML_n to Give an Imprinted Polymer **P3**

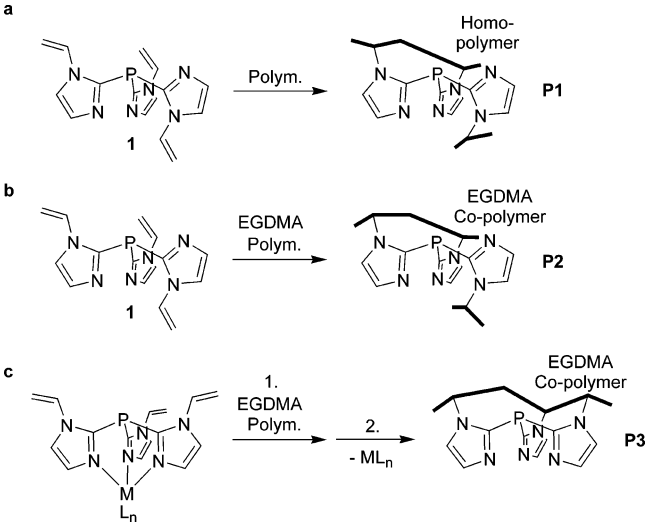

rene beads,[6] or incorporated into organic polymers by copolymerization with divinylbenzene,[7,8] ethyleneglycol dimethacrylate (EGDMA),[8,9] or trimethylolpropane trimethacrylate.[10] In the presence of Cu^{2+} ions, strong hydrolytic activity was observed with model substrates such as (*p*-nitrophenyl)phosphates or diaryl carbonates.[11] Here, we describe a new approach, which is based on the immobilization of the tripodal *N*,*N*′,*N*′′-chelate ligand **1**. Three different polymers were prepared in order to evaluate the influence of some key parameters such as site density of the metal centers and preorganization of the copper binding site. Polymer **P1** was generated by homopolymerization of the chelate ligand **1** (Scheme 1a). The trifunctional monomer **1** should lead to extensive cross-linking and therefore to a polymer with a very high density of rigid binding sites containing a variable number of N-donor groups. A disadvantage of such a polymer is that, after incorporation of Cu^{2+}, some of the metal centers are saturated by N-donor ligands and thus are catalytically inactive. A possible advantage, on the other hand, is that the high metal concentration could lead to multinuclear reaction centers, which might facilitate hydrolysis reactions due to cooperative effects.[4]

Polymer **P2** was prepared by copolymerization of ligand **1** with EGDMA (Scheme 1b). The lower concentration of the ligand with respect to the cross-linker EGDMA (77 mol %) should lead to mostly site-isolated binding sites, which reduces the probability Cu(μ-OH)$_2$Cu dimer formation but also of cooperative effects. It should be anticipated, however, that the conformation of some ligands is restrained in such a fashion that a tridentate coordination to Cu^{2+} is not possible (as shown in Scheme 1b). To ensure that the conformation of the immobilized ligand is fixed so that it can act as a highly preorganized tridentate *N*,*N*′,*N*′′-chelate, we have also employed a metal complex of ligand **1** as the monomer (Scheme 1c). This metal fragment ML_n acts as a template to molecularly imprint[12] the ideal conformation of the ligand. After polymerization, it is exchanged by the catalytically active Cu^{2+}. In the following, the synthesis and the characterization of these polymers is described. Furthermore, their ability to promote hydrolysis reactions of activated phosphoesters is evaluated.

Scheme 2. Synthesis of the Tripodal *N*,*N*′,*N*′′-Chelate Ligand **1**

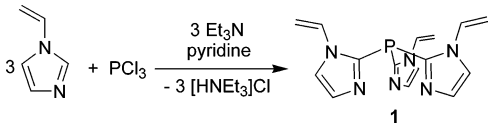

Results and Discussion

Synthesis of the Polymerizable *N*,*N*′,*N*′′-Chelate Ligand 1. The chelate ligand **1** was chosen as the functional monomer for several reasons: (a) its nitrogen donors are of the imidazolyl type, mimicking the histidine side chains found in the binding sites of many hydrolytic metalloenzymes; (b) it contains three vinyl groups and polymerization is expected to result in a rigid, highly cross-linked polymer; (c) as outlined below, ligand **1** can be prepared in a single step from commercially available starting materials, which allows generation of larger quantities; (d) reactions can be easily followed by ^{31}P NMR spectroscopy.

The synthesis of tertiary phosphines with heterocyclic substituents starting from lithiated or trimethylsilylated imidazoles was reported in 1982.[13] More recently, direct C-2 phosphorylation of 1-alkylimidazoles in pyridine/triethylamine was intruduced as an alternative route to tris[2-(1-alkylimidazolyl)]phosphines.[14] Following this approach by using 1-vinylimidazole, it was possible to obtain tris[2-(1-vinylimidazolyl)]phosphine **1** in 29% yield (Scheme 2). The ^{1}H and ^{13}C NMR spectra of **1** were in accordance with a C_{3v} symmetrical structure. The chemical shift of the ^{31}P NMR signal of **1** ($\delta = -58.89$ ppm) was very similar to that of tris[2-(1-methylimidazolyl)]phosphine ($\delta = -58.7$ ppm),[14] indicating the close relationship of both. The molecular

(5) Bodsgard, B. R.; Burstyn, J. N. *Chem. Commun.* **2001**, 647−648.
(6) Menger, F. M.; Tsuno, T. *J. Am. Chem. Soc.* **1989**, *111*, 4903−4907.
(7) Chandrasekhar, V.; Athimoolam, A.; Srivatsan, S. G.; Sundaram, P. S.; Verma, S.; Steiner, A.; Zacchini, S.; Butcher, R. *Inorg. Chem.* **2002**, *41*, 5162−5173.
(8) (a) Srivatsan, S. G.; Parvez, M.; Verma, S. *Chem. Eur. J.* **2002**, *8*, 5184−5191. (b) Srivatsan, S. G.; Verma, S. *Chem. Eur. J.* **2001**, *7*, 828−833. (c) Srivatsan, S. G.; Verma, S. *Chem. Commun.* **2000**, 515−516.
(9) Liu, J.-Q.; Wulff, G. *J. Am. Chem. Soc.* **2004**, *126*, 7452−7453.
(10) (a) Hartshorn, C. M.; Deschamps, J. R.; Singh, A.; Chang, E. L. *React. Funct. Polym.* **2003**, *55*, 219−229. (b) Hartshorn, C. M.; Singh, A.; Chang, E. L. *J. Mater. Chem.* **2002**, *12*, 602−605. (c) Lu, Q.; Singh, A.; Deschamps, J. R.; Chang, E. L. *Inorg. Chim. Acta* **2000**, *309*, 82−90.
(11) For immobilized Cu(II) complexes with peptidase activity see: Suh, J. *Acc. Chem. Res.* **2003**, *36*, 562−570.
(12) For reviews about molecular imprinting with transition metal complexes see: (a) Becker, J. J.; Gagne, M. R. *Acc. Chem. Res.* **2004**, *37*, 798−804. (b) Tada, M.; Iwasawa, Y. *J. Mol. Catal. A* **2003**, *199*, 115−137. (c) Alexander, C.; Davidson, L.; Hayes, W. *Tetrahedron* **2003**, *59*, 2025−2057. (d) Wulff, G. *Chem. Rev.* **2002**, *102*, 1−28. (e) Severin, K. *Curr. Opin. Chem. Biol.* **2000**, *4*, 710−714.
(13) Moore, S. S.; Whitesides, G. M. *J. Org. Chem.* **1982**, *47*, 1489−1493.
(14) Tolmachev, A. A.; Yurchenko, A. A.; Merculov, A. S.; Semenova, M. G.; Zarudnitskii, E. V.; Ivanov, V. V.; Pinchuk, A. M. *Heteroatom Chem.* **1999**, *10*, 585−597.

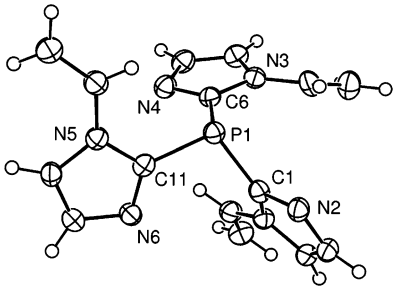

Figure 1. ORTEP[15] representation of the molecular structure of ligand **1** in the crystal. The solvent molecule ($0.5C_6H_6$) is omitted for clarity. Selected bond lengths (Å) and angles (deg): P1−C1 = 1.813(2), P1−C6 = 1.825(2), P1−C11 = 1.827(2); C1−P1−C6 = 101.73(10), C1−P1−C11 = 102.24(10), C6−P1−C11 = 98.39(10).

Scheme 3. Formation of the Sandwich-type Complexes **2** and **3**

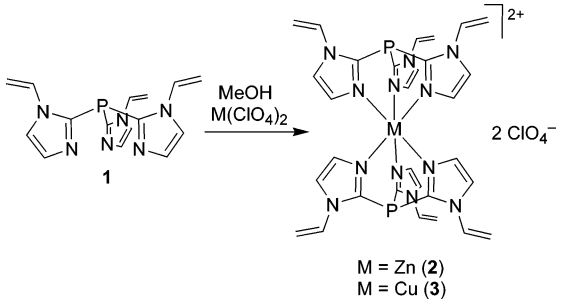

structure of **1** was confirmed by single-crystal X-ray crystallography (Figure 1).

The phosphorus atom of **1** shows the expected trigonal pyramidal geometry. The P−C bond lengths (1.813(2)−1.827(2) Å) and the C−P−C bond angles (98.39(1)−102.24(1)°) are similar to those found for tris[2-(1-methyl-4-tolylimidazolyl)]phosphine.[16] Ligand **1** exhibits the chiral propeller arrangement often seen in triarylphosphines.[16,17] With respect to the plane defined by the N-donor atoms N2, N4, and N6, two of the vinyl groups are pointing "up" and one "down". If such a conformation would be fixed by polymerization, the immobilized ligand would not be able to act as a tridentate *N*,*N*′,*N*″-ligand. In solution, however, a fast rotation around the P−C bonds of **1** is possible as evidenced by the ^{1}H and ^{13}C NMR spectra.

Metal Complexes of Ligand 1. To prepare the imprinted polymer **P3**, we have investigated the coordination chemistry of ligand **1.** When simple late transition metal salts were employed, the formation of sandwich-type complexes of low solubility was observed (Scheme 3). Upon addition of $M(ClO_4)_2$ salts (M = Zn, Cu) to a methanol solution of **1**, for example, precipitates of $[M(\mathbf{1})_2](ClO_4)_2$ (**2**, **3**) were formed as evidenced by single-crystal X-ray crystallography (**2**), NMR spectroscopy (**2**), and elemental analyses (**2** and **3**). Precipitates were also observed when the chloride salts $ZnCl_2$ and $CuCl_2$ were employed. These results were not unexpected since facial-capping trinitrogen ligands are known to form stable sandwich-type complexes with zinc[18] or copper ions.[19]

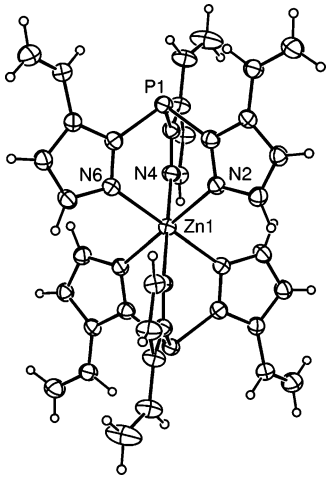

Figure 2. ORTEP[15] representation of the molecular structure of the cation of complex **2** in the crystal. The solvent molecules ($2CH_3OH$; $0.5H_2O$) and anions are omitted for clarity. Selected bond lengths (Å) and angles (deg): Zn1−N2 = 2.192(3), Zn1−N4 = 2.130(3), Zn1−N6 = 2.186(3); N4−Zn1−N6 = 86.91(13), N4−Zn1−N2 = 86.47(13), N6−Zn1−N2 = 86.50(13).

The molecular structure of **2** in the crystal confirmed the expected octahedral geometry of the cation $[Zn(\mathbf{1})_2]^{2+}$ (Figure 2). The Zn−N bond distances (2.130(3)−2.192(3) Å) and the N−Zn−N bond angles related to the asymmetric unit (86.5(1)−86.9(1)°) are comparable to those found for the cation $[Zn\{P(C_5H_4N)_3\}_2]^{2+}$.[19c]

Whereas complex **3** displayed a very low solubility in all solvents tested, complex **2** was moderately soluble in acetone. The spectra of **2** in acetone-d_6 showed only one set of signals. A pronounced difference in chemical shifts compared to the free ligand **1** was found for the ^{31}P NMR signal of **2**, for which an upfield shift of 60 ppm was observed ($\delta = -119.76$ ppm).

Searching for a metal complex, which would react with ligand **1** in a defined 1:1 ratio, we next focused on η^3-allyldicarbonylmolybdenum complexes. These organometallic complexes are known to form stable adducts with tridentate ligands such as histidine[20] and hydrotris(1-pyrazolyl)borate.[21] Starting from the neutral chloro complexes $[Mo(\eta^3\text{-}C_3H_4R)Cl(CH_3CN)_2(CO)_2]$ (R = H, CH_3),[22] we first prepared the cationic trisacetonitrile complexes [Mo(η^3-

(15) Farrugia, L. J. *J. Appl. Crystallogr*. **1997**, *30*, 565.
(16) Kläui, W.; Piefer, C.; Rheinwald, G.; Lang, H. *Eur. J. Inorg. Chem.* **2000**, 1549−1555.
(17) Copping, D.; Frampton, C. S.; Howard-Lock, H. E.; Lock, C. J. L. *Acta Crystallogr*. **1992**, *C48*, 675−677.
(18) (a) Parkin, G. *Chem. Rev.* **2004**, *104*, 699−768. (b) Vahrenkamp, H. *Acc. Chem. Res.* **1999**, *32*, 589−596.
(19) (a) Jonas, R. T.; Stack, T. D. P. *Inorg. Chem.* **1998**, *37*, 6615−6629. (b) Astley, T.; Ellis, P. J.; Freeman, H. C.; Hitchman, M. A.; Keene, F. R.; Tiekink, E. R. T. *J. Chem. Soc., Dalton Trans.* **1995**, 595−601. (c) Astley, T.; Headlam, H.; Hitchman, M. A.; Keene, F. R.; Pilbrow, J.; Stratemeier, H.; Tiekink, E. R. T.; Zhong, Y. C. *J. Chem. Soc., Dalton Trans.* **1995**, 3809−3818. (d) Hegetschweiler, K.; Gramlich, V.; Ghisletta, M.; Samaras, H. *Inorg. Chem.* **1992**, *31*, 2341−2346. (e) Chaudhuri, P.; Oder, K.; Wieghardt, K.; Weiss, J.; Reedijk, J.; Hinrichs, W.; Wood, J.; Ozarowski, A.; Stratemaier, H.; Reinen, D. *Inorg. Chem.* **1986**, *25*, 2951−2958. (f) Ammeter, J.; Buergi, H. B.; Gamp, E.; Meyer-Sandrin, V.; Jensen, W. P. *Inorg. Chem.* **1979**, *18*, 733−750. (g) Fry, F. H.; Jensen, P.; Kepert, C. M.; Spiccia, L. *Inorg. Chem.* **2003**, *42*, 5637−5644.
(20) van Staveren, D. R.; Bill, E.; Bothe, E.; Bühl, M.; Weyhermüller, T.; Metzler-Nolte, N. *Chem. Eur. J.* **2002**, *8*, 1649−1662.
(21) (a) Ward, Y. D.; Villanueva, L. A.; Allred, G. D.; Payne, S. C.; Semones, M. A.; Liebeskind, L. S. *Organometallics* **1995**, *14*, 4132−4156. (b) Trofimenko, S. *J. Am. Chem. Soc.* **1969**, *91*, 588−595.
(22) Dieck, H. T.; Friedel, H. *J. Organomet. Chem.* **1968**, *14*, 375−385.

Scheme 4. Synthesis of the Molybdenum Complexes **4** and **5**

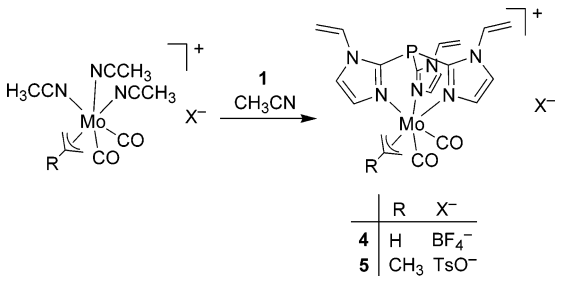

	R	X^-
4	H	BF_4^-
5	CH_3	TsO^-

$C_3H_4R)(CH_3CN)_3]X$[23] by reaction with silver tetrafluoroborate or silver tosylate in acetonitrile. Without isolation, they were reacted directly with ligand **1** (Scheme 4). The desired complexes **4** and **5** were isolated by concentration of the resulting solution followed by precipitation with diethyl ether.

Both complexes were comprehensively characterized by NMR and IR spectroscopy, elemental analysis, and X-ray crystallography. The infrared spectra showed strong bands for the carbonyl ligands at $\nu_{CO} = 1943/1855$ cm^{-1} (**4**) and $\nu_{CO} = 1935/1836$ cm^{-1} (**5**), respectively. These values are similar to what has been observed for the structurally related hydrotris(1-pyrazolyl)borato complexes.[21] Upon coordination to the Mo(η^3-allyl)$(CO)_2$ fragment, the three vinylimidazole groups of ligand **1** are no longer equivalent. This reduced symmetry was manifested in the ^{1}H NMR spectra of the complexes **4** and **5** (CD_3CN). The allyl or methallyl ligands showed no fluxional *endo*/*exo* dynamic on the NMR time scale at room temparature.[24] As was found for complex **2**, the ^{31}P NMR signals of **4** and **5** exhibited a characteristic upfield shift (**4**: $\delta = -112.28$ ppm; **5**: $\delta = -111.93$ ppm) compared to the free ligand **1**.

Single crystals were obtained by slow diffusion of diethyl ether into concentrated solutions of **4** and **5** in acetonitrile. Considering the allyl or methallyl ligand as a single substituent, the complexes possess a six-coordinate octahedral geometry (Figures 3 and 4). With respect to the $Mo(CO)_2$ unit, the allyl ligands adopt an *exo* conformation in which the central carbon atoms points "up" to the *N*,*N*′,*N*″-chelate ligand. The bond lengths and angles found for **4** and **5** are within the expected range and similar to those found for [Mo(η^3-allyl)(Tp)$(CO)_2$].[21a]

Synthesis of the Polymers. Radical initiated homopolymerization of **1** in methanol at 65 °C gave the insoluble, pale yellow polymer **P1** in high yield (88%). The polymer was ground, washed with MeOH, and then suspended in a solution of anhydrous $CuCl_2$ in methanol (Scheme 5). Immediately, a color change to dark green was observed, indicating an easy access to the metal binding sites. After 20 min, the metalated polymer **P1**−**Cu** was isolated, washed extensively with MeOH, and dried. The metal content was found to be 126 mg of Cu/g of polymer as determined by ICP-OES. This corresponds to an occupation rate of 67% of all *N*,*N*′,*N*″-sites. Analysis of **P1**−**Cu** by IR spectroscopy showed a small band at $\nu = 1644$ cm^{-1}. This band can be attributed to the remaining vinyl groups, which were not polymerized. The polymeric backbone of **P1**−**Cu** was thus expected to show a certain flexibility.

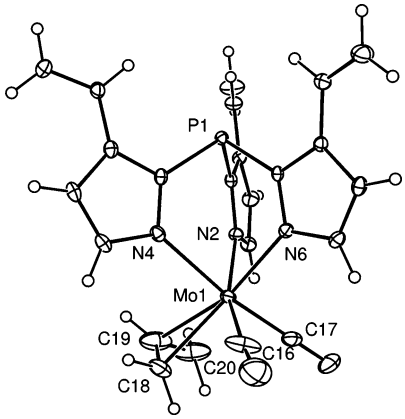

Figure 3. ORTEP[15] representation of the molecular structure of the cation of complex **4** in the crystal. The anion is omitted for clarity. Selected bond lengths (Å) and angles (deg): Mo1−N2 = 2.267(3), Mo1−N4 = 2.325(3), Mo1−N6 = 2.241(3), Mo1−C16 = 1.977(5), Mo1−C17 = 1.951(4), Mo1−C18 = 2.345(4), Mo1−C19 = 2.220(5), Mo1−C20 = 2.404(6); N6−Mo1−N4 = 80.96(10), N2−Mo1−N4 = 83.96(10), N6−Mo1−N2 = 78.97(10), C17−Mo1−C16 = 82.7(2).

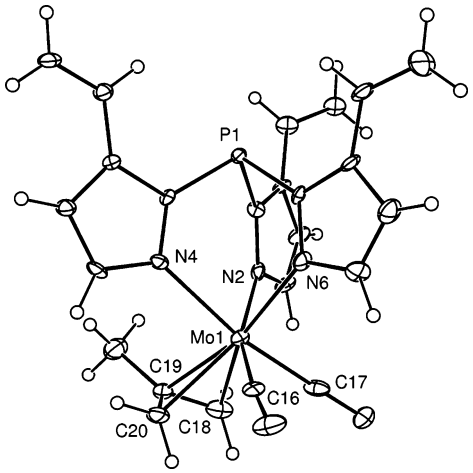

Figure 4. ORTEP[15] representation of the molecular structure of the cation of complex **5** in the crystal. The solvent molecule ($0.5Et_2O$) and the anion are omitted for clarity. Selected bond lengths (Å) and angles (deg): Mo1−N2 = 2.272(6), Mo1−N4 = 2.319(6), Mo1−N6 = 2.246(6), Mo1−C16 = 1.886(10), Mo1−C17 = 1.933(8), Mo1−C18 = 2.352(8), Mo1−C19 = 2.266(8), Mo1−C20 = 2.304(8); N2−Mo1−N4 = 84.1(2), N6−Mo1−N2 = 81.1(2), N6−Mo1−N4 = 79.5(2), C16−Mo1−C17 = 76.7(3).

In a related fashion, the polymer **P2**−**Cu** was obtained by copolymerization of ligand **1** (23 mol %) with the crosslinker EGDMA (77 mol %) and subsequent metalation with $CuCl_2$ (Scheme 5). The metal content of **P2**−**Cu** was found to be 46 mg of Cu/g of polymer, which corresponds to an occupation rate of approximately 76% of all *N*,*N*′,*N*″-sites.

To generate a polymer **P3** with a conformationally imprinted binding site, we have copolymerized the molybdenum complex **4** or **5** (23 mol %) with EGDMA (77 mol %) in acetonitrile. Surprisingly, the two complexes gave very different results. For reaction mixtures containing the allyl complex **4**, a black solution was obtained after 24 h at 65

(23) (a) Brisdon, B. J.; Cartwright, M.; Hodson, A. G. *J. Organomet. Chem.* **1984**, *277*, 85−90. (b) Brisdon, B. J.; Cartwright, M. *J. Organomet. Chem.* **1979**, *164*, 83−96.

(24) Fluxionality in diamagnetic complexes of the general formula [(η^3-allyl)$(CO)_2ML_2X$] (M = Cr, Mo, W) has been studied in detail by NMR spectroscopy. See ref 20.

Scheme 5. Synthesis of the Copper-Containing Polymers **P1**−**Cu** and **P2**−**Cu**

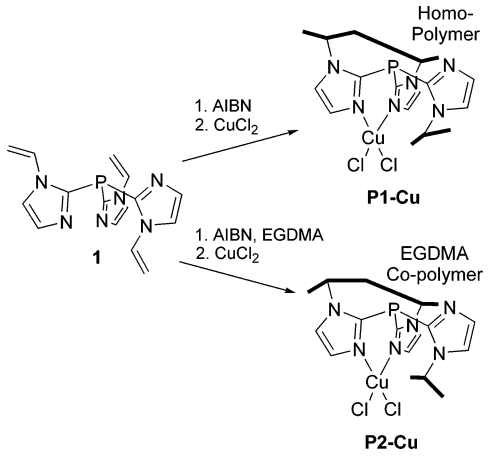

Scheme 6. Synthesis of the Copper-Containing Polymer **P3**−**Cu**

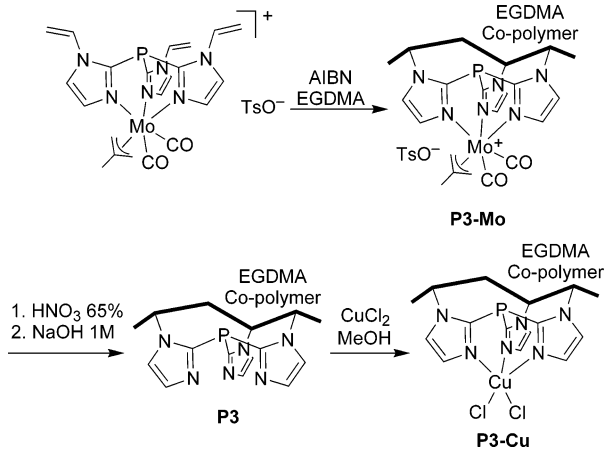

°C, indicating inhibition of the polymerization and decomposition of the complex. In contrast, reactions of the methallyl complex **5** resulted in clean polymerization: after 24 h, the yellow polymer **P3**−**Mo** could be isolated in 81% yield (Scheme 6).

When the polymer **P3**−**Mo** was washed with acetonitrile, the solution was slightly colored. Analysis of this solution by ^{31}P NMR spectroscopy revealed the presence of nonpolymerized complex **5**. This result showed that complex **5** was indeed stable during the polymerization process, but it also suggested that the incorporation of the complex in the polymer was not quantitative. This was confirmed by ICP-OES: the molybdenum content of **P3**−**Mo** was 26 mg of Mo/g of polymer, which corresponds to an incorporation rate of 38%. The IR spectrum of **P3**−**Mo** showed two CO bands at ν_{CO} = 1939 and 1847 cm^{-1} (Figure 5). These values are similar to what was found for the free complex **5** (ν_{CO} = 1935/ 1836 cm^{-1}), indicating the structural integrity of the molybdenum complex during the immobilization process.

The "dummy metal template" [Mo(η^3-C$_4$H$_7$)(CO)$_2$]$^+$ was cleaved off by treating the polymer **P3**−**Mo** for 30 min with concentrated HNO_3 (65%). The polymer was subsequently neutralized with aqueous NaOH (1 M) to give **P3** (Scheme 6). To verify that the phosphine chelate ligand tolerates these conditions, ligand **1** was incubated for 30 min in HNO_3 (65%). The ^{31}P NMR spectrum of the resulting solution

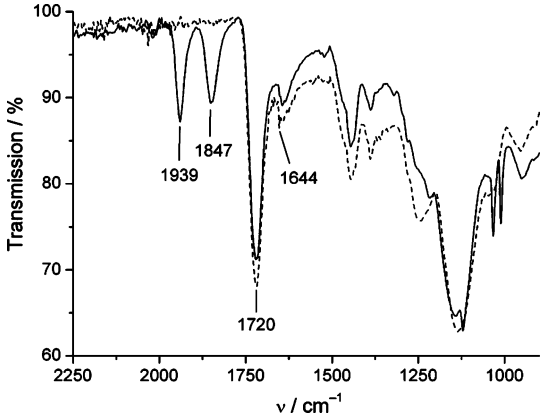

Figure 5. IR spectra of the polymers **P3**−**Mo** (solid line) and **P3**−**Cu** (dotted line).

showed only one signal at $\delta = -83.02$ ppm, which can be attributed to the protonated ligand **1**.[25] No change in the ^{31}P NMR spectrum was observed when a methanolic solution of **1** was mixed with aqueous NaOH (1 M). From these experiments it was concluded that the immobilized ligand **1** tolerates both the short treatment with concentrated HNO_3 as well as the neutralization with base.

After extensive washing, polymer **P3** was suspended in a methanol solution of anhydrous $CuCl_2$ (Scheme 6). As was observed for **P1** and **P2**, an immediate color change to dark green was observed. The metalated polymer **P3**−**Cu** was found to contain 30 mg of Cu/g of polymer and 7 mg of Mo/g of polymer (ICP-OES). This showed that 73% of the Mo complexes of **P3**−**Mo** were removed by the treatment with nitric acid and that the liberated binding sites were efficiently re-occupied by $CuCl_2$. The removal of the [Mo(η^3-C$_4$H$_7$)(CO)$_2$]$^+$ complexes was furthermore confirmed by IR spectroscopy: no CO bands were observed in the IR spectrum of **P3**−**Cu** (Figure 5).

Methanol and water easily wetted the hydrophilic polymers **P1**−**Cu**, **P2**−**Cu**, and **P3**−**Cu**. The swelling ratio Q in water at room temperature (measured by volume increase of wetted polymers) was 1.5 (**P1**−**Cu**), 1.1 (**P2**−**Cu**), and 1.9 (**P3**−**Cu**), respectively. The addition of water was expected to lead to a replacement of the chloro ligands by aqua ligands. For the polymers **P1**−**Cu** and **P2**−**Cu**, this ligand exchange was accompanied by a color change from green to blue within one minute. The color of the polymer **P3**−**Cu**, however, did not change significantly. Prolonged incubation of the polymers **P1**−**Cu** and **P2**−**Cu** into an aqueous CHES buffer solution at pH 9.0 resulted in a color change from blue to black (CuO) after ∼12 h, while no change of color was found for **P3**−**Cu**. These experiments point to the fact that the copper complexes in **P1**−**Cu** and **P2**−**Cu** exhibit a different coordination environment and a lower stability than the complexes in polymer **P3**−**Cu**.

To probe the copper(II) environments in the polymers, powder X-band EPR spectra of **P1**−**Cu**, **P2**−**Cu**, and **P3**−**Cu** were recorded at 70 K. The homopolymer **P1**−**Cu** (Figure 6) gave rise to a broad symmetric spectrum with no

(25) This was evidenced by control reactions of **1** with HBF_4 (50%), for which the same signal was observed.

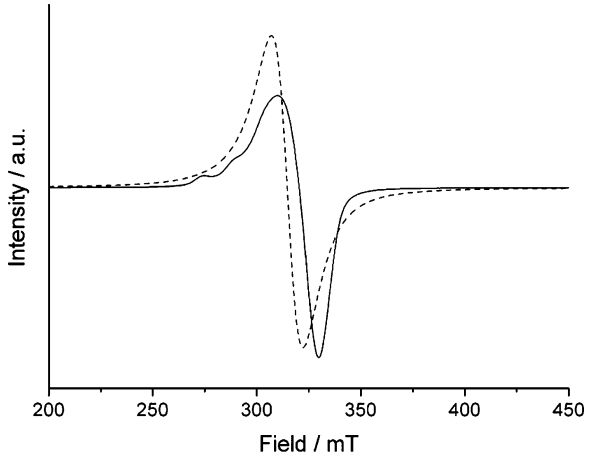

Figure 6. X-band powder EPR spectra of **P1**−**Cu** (dotted line) and **P3**−**Cu** (solid line) at 70 K.

hyperfine coupling due to spin−spin interactions between the copper centers ($g = 2.13$). This can be explained by the high density of structurally heterogeneous copper complexes in **P1**−**Cu**, which results in a collapse of the hyperfine structure.[26] In contrast, the spectra of the polymers **P2**−**Cu** (not shown) and **P3**−**Cu** (Figure 6) displayed a partially resolved hyperfine structure, indicating reduced spin−spin interactions and greater distances between the copper centers (Figure 6). The *g*-factors observed for these polymers are $g = 2.11$ (**P2**−**Cu)** and $g = 2.10$ (**P3**−**Cu)**.

Hydrolysis Reactions. To evaluate the hydrolytic activity of the polymers **P1**−**Cu**, **P2**−**Cu**, and **P3**−**Cu**, we investigated the hydrolysis of the activated phosphodiesters bis(*p*-nitrophenyl)phosphate (BNPP) and (*p*-nitrophenyl)phosphate (NPP). These substrates are frequently used as models for biologically relevant phosphoesters such as RNA and DNA. Advantages and drawbacks of such activated model substrates have been discussed by Breslow and Singh[27] and Menger and Ladika.[28]

The reactions were performed in buffered aqueous solution at room temperature. The amount of polymer that was employed corresponds to a Cu^{2+} concentration of 1.0 mM if the polymers would be completely soluble in the buffer. After an incubation time of 30 min, the reactions were initiated by addition of a freshly prepared stock solution of the substrate BNPP or NPP (final concentration: 5.0 mM). After a given time, the reaction tubes were centrifuged and the concentration of the product *p*-nitrophenolate was determined by UV/Vis spectroscopy at $\lambda = 400$ nm. No correction for background hydrolysis was performed as it can be considered negligible.[29]

All three polymers displayed a strong hydrolytic activity. The pseudo-first-order rate constants for the hydrolysis of BNPP was found to depend on the polymer as well as on the reaction conditions and varied between 6.0×10^{-5} and 1.3×10^{-3} min^{-1} (Table 1). This is approximately 5 orders of magnitude faster than the background reaction without polymer[29] and comparable to what has been observed for some of the most active immobilized Cu complexes.[7,8,10] Of special interest were the differences in reactivity of the three polymers. For the hydrolysis of BNPP, the activity increases in the order **P2**−**Cu** < **P1**−**Cu** < **P3**−**Cu**. The molecularly imprinted copolymer **P3**−**Cu** with a defined *N*,*N*′,*N*″ binding site was 9 times more active than the copolymer **P2**−**Cu** with less uniform copper binding sites but otherwise identical composition. The homopolymer **P1**−**Cu** was found to be more active than the nonimprinted copolymer **P2**−**Cu**. The reason for this difference in activity could be due some cooperative effects of adjacent Cu^{2+} centers in **P2**−**Cu**, but variations in the chemical composition and/or the morphology of the polymers could also affect the hydrolysis rates. An intrinsic advantage of the homopolymer **P1**−**Cu** is the fact that due to the high Cu^{2+} content of 126 mg of Cu/g of polymer, only very small amounts of the polymer are needed to promote the hydrolysis reaction.

Table 1. Pseudo-First-Order Rate Constants (min^{-1}) for the Hydrolysis of BNPP and NPP by **P1**−**Cu**, **P2**−**Cu**, and **P3**−**Cu**[a]

	HEPES, H_2O	*N*-ethylmorpholine, 34% aq MeOH	
polymer	BNPP	BNPP	NPP
P1−**Cu**	3.7×10^{-4}	2.0×10^{-4}	2.9×10^{-4}
P2−**Cu**	6.0×10^{-5}	1.5×10^{-4}	3.1×10^{-4}
P3−**Cu**	5.3×10^{-4}	1.3×10^{-3}	1.3×10^{-4}

[a] Reaction conditions: $[Cu^{2+}] = 1.0$ mM, [BNPP] or [NPP] = 5.0 mM, 70 mM buffer, pH 7.8, 25 °C. Reactions were monitored to less than 5% conversion of the substrate. Rate constants were calculated from the $-\ln(1 - A/A_{max})$ versus time plots. Averaged values from two independent experiments are given; the errors are less than 4%.

To make sure that diffusional processes were not rate limiting in these reactions, we have investigated the hydrolysis of BNPP in aqueous buffer solution using polymers with a different average particle size (>100 μm and 25−50 μm). For all three polymers, the rates were the same for the two batches. This result was in agreement with the observation that the stirring speed had a negligible effect on the hydrolysis rates as long as the polymer particles were homogeneously suspended in the solution.

The pseudo-first-order rate constants for the hydrolysis of the monoester NPP were found to vary between 1.3×10^{-4} and 3.1×10^{-4} min^{-1} (Table 1). The values are thus similar to what was observed in the hydrolysis of the diester BNPP. It is interesting to note that for Cu−triazacyclononane complexes, the hydrolysis of NPP is generally around 50−500 times slower than the hydrolysis of BNPP.[3] This difference in activity could be due to the formation of catalytically inactive dinuclear complexes with bridging NPP ligands as characterized by Spiccia et al.[3c] The formation of such complexes is less likely for the immobilized copper complexes in **P1**−**Cu**, **P2**−**Cu**, and **P3**−**Cu**, which could

(26) (a) Sanmartín, J.; Bermejo, M. R.; García-Deibe, A. M.; Nascimento, O. R.; Lezama, L.; Rojo, T. *J. Chem. Soc., Dalton Trans.* **2002**, 1030−1035. (b) Brondino, C. D.; Calvo, R.; Baran, E. J. *Chem. Phys. Lett.* **1997**, *271*, 51−54. (c) Rojo, T.; lnsausti, M.; Lezama, L.; Pizarro, J. L.; Arriortua, M. I.; Calvo, R. *J. Chem. Soc., Faraday Trans.* **1995**, *91*, 423−426. (d) Calvo, R.; Passeggi, M. C. G.; Novak, M. A.; Symko, O. G.; Oseroff, S. B.; Nascimento, O. R.; Terrile, M. C. *Phys. Rev. B* **1991**, *43*, 1074−1083.

(27) Breslow, R.; Singh, S. *Bioorg. Chem.* **1988**, *16*, 408−417.

(28) Menger, F. M.; Ladika, M. *J. Am. Chem. Soc.* **1987**, *109*, 3145−3146.

(29) The rate of the spontaneous hydrolysis of BNPP at pH 7 and 25 °C has been estimated to be 1×10^{-11} s^{-1}. See: Livieri, M.; Mancin, F.; Tonellato, U.; Chin, J. *Chem. Commun.* **2004**, 2862−2863.

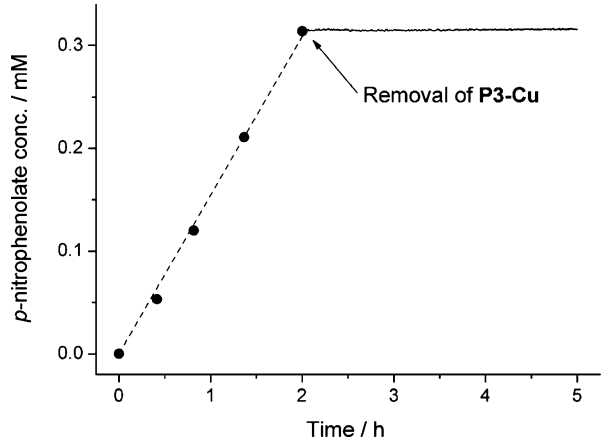

Figure 7. Plot of *p*-nitrophenolate concentration versus time for the **P3**−**Cu**-mediated hydrolysis of BNPP. Reaction conditions: $[Cu^{2+}] = 1.0$ mM, [BNPP] = 5.0 mM, H_2O, 70 mM HEPES buffer, pH 7.8, 25 °C. The data points represent averaged values form two independent experiments; the errors are less than 4%.

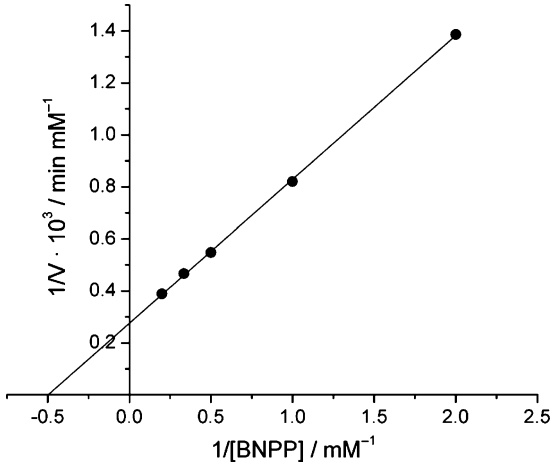

Figure 8. Lineweaver-Burk plot for **P3**−**Cu**-mediated hydrolysis of BNPP as a function of substrate concentration. Reaction conditions: $[Cu^{2+}] = 1.0$ mM, [BNPP] = 0.5−5.0 mM, H_2O, 70 mM HEPES buffer, pH 7.8, 25 °C. The data points represent averaged values form two independent experiments; the errors are less than 4%.

explain the increased relative activity for the hydrolysis of NPP as compared to BNPP.

The activities for the hydrolysis of NPP increases in the order **P3**−**Cu** < **P1**−**Cu** ∼ **P2**−**Cu**. This trend is different from what has been observed for the hydrolysis of BNPP. Apparently, the formation of a structurally defined *N*,*N*′,*N*″ binding site by molecular imprinting is less suited for the hydrolysis of the monoester NPP. The divalent *N*,*N*′ binding sites, which are believed to be present in **P1**−**Cu** and **P2**−**Cu** but not in **P3**−**Cu**, could therefore be beneficial for the reaction but the heterogeneity of the polymers **P1**−**Cu** and **P2**−**Cu** hampers a more precise conclusion.

Under the reaction conditions (70 mM HEPES buffer, pH 7.8, 25 °C), leaching of Cu^{2+} into the solution was found to be low for all polymers (∼5% as determined by ICP-OES). At pH 5−6, however, significantly higher values were determined, especially for **P1**−**Cu** and **P2**−**Cu**. Kinetic experiments at pH < 7.0 were thus not performed. To verify that immobilized copper complexes were responsible for catalysis and not the small amounts of leached Cu^{2+}, we have performed "stop-experiments" in which the polymer was separated after 2 h by centrifugation and the isolated supernatant was monitored spectrophotometrically. The hydrolysis reaction of BNPP was slowed significantly by a factor of 500, as is shown for **P3**−**Cu** in Figure 7. The copper-free polymers **P1**, **P2**, **P3**, and **P3**−**Mo** showed no acceleration of the hydrolysis of BNPP or NPP at all.

Attempts to quantify the hydrolysis activity of a mixture of ligand **1** and $CuCl_2$ in homogeneous solution were hindered by the fact that **1** displays a very low solubility in plain water. In a solution containing 50% methanol (HEPES buffer, pH 7.8), ligand **1** was only partially soluble and precipitation of $[Cu(OH)_2]$ occurred. In pure methanol, the formation of sandwich-type complexes of low solubility was observed as described above. An evaluation of the hydrolytic activity of Cu^{2+} complexes of ligand **1** in homogeneous solution was thus not possible.

The hydrolysis of BNPP promoted by the imprinted polymer **P3**−**Cu** was investigated in more detail. In experiments with a variable substrate concentration, saturation behavior was observed ([BNPP] = 0.5−5.0 mM, $[Cu^{2+}] = 1.0$ mM). From the corresponding Lineweaver−Burk plot (Figure 8), the following Michaelis−Menten parameters were determined: $K_M = 2.0$ mM, $V_{max} = 3.6 \times 10^{-3}$ mM min^{-1} and $k_{cat} = 3.6 \times 10^{-3}$ min^{-1}.[30] The catalytic efficiency was $k_{cat}/K_M = 1.8 \times 10^{-3}$ mM^{-1} min^{-1}. This is about 1 order of magnitude higher than what was found for copper complexes of immobilized phosphazene[7] or nucleobase ligands[8a] under related conditions.

The polymer **P3**−**Cu** was able to act as a true catalyst, as evidenced by the fact that *p*-nitrophenolate was observed in 35% yield after 30 h using a substrate-to-catalyst ratio of 5:1. For this reaction, it is likely that some hydrolysis of the reaction product NPP occurred concomitantly to the hydrolysis of BNPP.[31]

The effect of pH on the hydrolytic activity of **P3**−**Cu** was studied in the pH range 7.0−9.0. An increase of the initial rates with an increase of pH was observed (Figure 9). It should be noted that a continuous increase above pH 8 is not common for homogeneous Cu(II) catalysts. In addition to the pH-rate profile, a potentiometric titration of **P3**−**Cu** was performed. The obtained data (Figure 10) indicated the presence of an acidic proton with an apparent pK_a ∼ 6.5.

Several mechanistic studies suggest that, for the phosphodiester hydrolysis with mononuclear Cu^{2+} complexes, an intramolecular attack on a complex-substrate intermediate by a metal-coordinated hydroxide is the crucial step.[4] A similar mechanism is likely to account for the hydrolytic activity of **P3**−**Cu**. Due to heterogeneity of the metal binding sites in **P1**−**Cu** and **P2**−**Cu**, a variety of reaction pathways are probably operational.

(30) At very high BNPP concentrations, a deviation from linearity was observed. This might be attributed to substrate inhibition as discussed in ref 10a.

(31) The data described in Table 1 and in the Figures 7−9 are based on initial rates (less than 5% conversion of BNPP). The concomitant hydrolysis of NPP can thus be neglected.

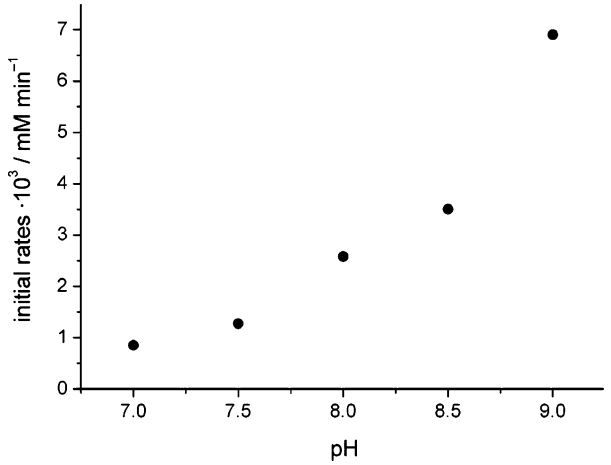

Figure 9. pH dependence of the **P3**−**Cu**-mediated hydrolysis of BNPP. Reaction conditions: $[Cu^{2+}] = 1.0$ mM, [BNPP] = 5.0 mM, H_2O, 25 °C, 70 mM buffer. The following buffers were employed: HEPES (pH 7.0), HEPPSO (pH 7.5−8.0), and CHES (pH 8.5−9.0).

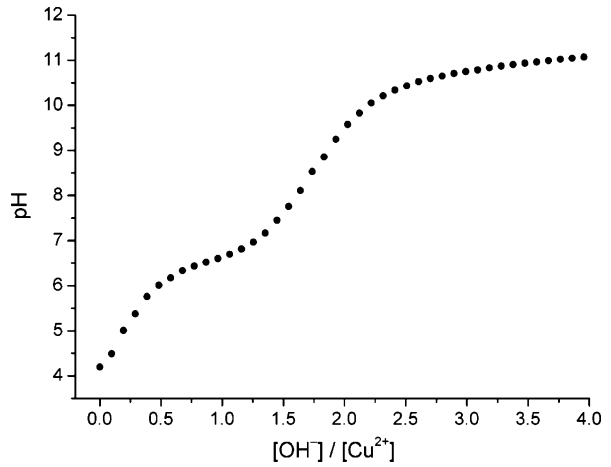

Figure 10. Potentiometric titration of **P3**−**Cu** in water with $CsOH_{aq}$.

Conclusion

Three different polymers containing the *N*,*N*′,*N*′′-chelate ligand **1** were prepared by (a) radical initiated homopolymerization of **1** (**P1**), (b) copolymerization of **1** with EGDMA (**P2**), or (c) molecular imprinting with the Mo complex **5** and EGDMA and subsequent removal of the "dummy" metal complex (**P3**). These polymers were used as high-loading supports for Cu^{2+}. Upon treatment with $CuCl_2$, the metalated polymers **P1**−**Cu**, **P2**−**Cu**, and **P3**−**Cu** were obtained. The concentration as well as the geometry of the copper complexes within the polymers was found to depend on the nature of the polymer. For the homopolymer **P1**−**Cu**, a very high metal content of 126 mg of Cu/g of polymer was determined. This corresponds to an occupation rate of 67% per *N*,*N*′,*N*′′ ligand. As expected, a lower value (46 mg/g) was found for the copolymer **P2**−**Cu** but, still, the accessibility of the binding sites in the highly cross-linked polymer was excellent. The lowest value was observed for the imprinted polymer **P3**−**Cu** (30 mg/g). The reduced copper content was found to be a result of an incomplete incorporation of the dummy metal complex **5** and a non-quantitative exchange of Cu for Mo. All three metalated polymers efficiently catalyzed the hydrolysis of the activated phosphoesters BNPP and NPP. Interestingly, the rates for the hydrolysis of the monoester NPP were nearly as high as those found for the diester BNPP. This is in accordance with results for other immobilized Cu(II) complexes[7,8a] but in contrast to what has been observed for several Cu(II) complexes with *N*,*N*′,*N*′′-chelate ligands in homogeneous solution.[3] It points to an intrinsic advantage of heterogeneous vs homogeneous catalysts. The relative activity of **P1**−**Cu**, **P2**−**Cu**, and **P3**−**Cu** was dependent on the substrate. For BNPP, the highest rates were observed for the imprinted polymer **P3**−**Cu** having a defined *N*,*N*′,*N*′′ binding site. For NPP, on the other hand, the polymers **P1**−**Cu** and **P2**−**Cu** gave slightly better results. This suggests that copper complexes with an alternative geometry (e.g., *N*,*N*′-chelate complexes) contribute to the observed hydrolytic activity. An interesting perspective for future studies is the possibility to use the technique of molecular imprinting to control not only the first- but also the second-coordination sphere of the hydrolytically active metal complex.[9,12] This would require the availability of polymerizable dummy metal complexes with substrate-analogue ligands. Current efforts in our laboratory are directed toward the synthesis of such complexes.

Experimental Section

General. The solvents (analytical-grade purity) were degassed and stored under a dinitrogen atmosphere. Sodium bis(*p*-nitrophenyl)phosphate (BNPP) and disodium (*p*-nitrophenyl)phosphate hexahydrate (NPP) were purchased at Sigma-Aldrich and Acros, respectively. Polymerizations were performed in a glovebox under an atmosphere of dinitrogen containing less than 1 ppm of oxygen and water. The synthesis of all organometallic complexes was performed under an atmosphere of dinitrogen using standard Schlenk techniques. The complexes $[Mo(\eta^3\text{-}C_3H_5)Cl(CH_3CN)_2(CO)_2]$ and $[Mo(\eta^3\text{-}C_4H_7)Cl(CH_3CN)_2(CO)_2]$ were prepared according to literature procedures.[22] Prior to utilization, 2,2′-azobisisobutyronitrile (AIBN) was re-crystallized from MeOH and ethyleneglycol dimethacrylate (EGDMA) was washed with NaOH (1 M) and saturated $NaCl_{aq}$ and dried over Na_2SO_4.

Instrumentation. The ^1H, ^{13}C, and ^{31}P spectra were recorded on a Bruker Advance DPX 400 or a Bruker Advance 200 spectrometer using the residual protonated solvents as internal standards (^1H, ^{13}C) or 85% H_3PO_4 as the external standard (^{31}P). All spectra were recorded at room temperature. The IR spectra were recorded on a Perkin-Elmer Spectrum One FT-IR spectrometer. The elemental analyses (Mo and Cu) were obtained by inductively coupled plasm atomic emission spectroscopy on a Perkin-Elmer ICP-OES 2000 DV instrument. Potentiometric titrations were performed with a Metrohm Titrino 716 DMS instrument. The pH measurements were carried out with a Metrohm 692 pH/ion meter. The EPR spectra were recorded in continuous-wave mode at X-band (9.4 GHz) on a Bruker eleXsys E 500 spectrometer at 70K using an ER 4112HV variable temperature cryostat. The Xepr software package was employed for all data acquisitions.

Synthesis. ***Warning***: Several compounds described in this work contain perchlorate anions. Although no accident has occurred, the use of perchlorate is hazardous because of the possibility of explosion, especially when compounds are anhydrous.

(a) Tris[2-(1-vinylimidazolyl)]phosphine (1). PCl_3 (4.61 mL, 52.8 mmol) was added to a stirred solution of 1-vinylimidazole

(14.5 mL, 158 mmol), NEt_3 (22.3 mL, 158 mmol), and pyridine (300 mL) at 0 °C. After the solution was stirred for 72 h at room temperature, the volatile components were removed in a vacuum and the beige residue was extracted with boiling benzene (200 mL). The yellow solution was filtered through activated carbon. Upon cooling, colorless crystals of crude **1** were formed. They were separated and re-crystallized twice from benzene (150 mL). Finally, the product was washed with benzene and diethyl ether and dried in a vacuum (yield: 5.08 g, 29%). ^{1}H NMR (400 MHz, MeOD): δ (ppm) = 4.89 (d, ^3J = 8 Hz, 3 H, CH=CH_2), 5.39 (d, ^3J = 16 Hz, 3 H, CH=CH_2), 7.09 (dd, ^3J_E = 16 Hz, ^3J_Z = 8 Hz, 3 H, CH=CH_2), 7.20 (s, 3 H, H_{Im}), 7.74 (s, 3 H, H_{Im}). ^{13}C NMR (101 MHz, MeOD): δ (ppm) = 105.51 (CH=*C*H_2), 122.32 (*C*H=CH_2), 130.67 (d, $^3J_{C-P}$ = 8 Hz), 132.28 (d, $^3J_{C-P}$ = 9 Hz), 140.77 (d, $^1J_{C-P}$ = 8 Hz). ^{31}P NMR (162 MHz, MeOD): δ (ppm) = −58.89. IR: ν (cm^{-1}) = 1644 (s, CH=CH_2). Anal. Calcd (%) for $C_{15}H_{15}N_6P\cdot{}^1/_3C_6H_6$: C, 60.71; H, 5.09; N, 24.99. Found: C, 60.72; H, 5.17; N, 24.27.

(b) [Zn(1)$_2$](ClO$_4$)$_2$ (2). $[Zn(OH_2)_6](ClO_4)_2$ (74.5 mg, 200 μmol) was added to a solution of ligand **1** (67.3 mg, 200 μmol) in methanol (10.0 mL). Colorless crystals were formed immediately. After 24 h, they were isolated, washed with methanol, and dried in a vacuum (yield: 73.2 mg, 40%). ^{1}H NMR (400 MHz, acetone-d_6): δ (ppm) 5.32 (d, ^3J = 8 Hz, 6 H, CH=CH_2), 5.76 (d, ^3J = 16 Hz, 6 H, CH=CH_2), 6.91 (s, 6 H, H_{Im}), 7.85−7.91 (m, 12 H, H_{Im} + CH=CH_2), 7.14 (s, 3 H, H_{Im}), 7.30 (s, 3 H, H_{Im}). ^{13}C NMR (101 MHz, acetone-d_6): δ (ppm) 106.65, 120.36 (d, $^3J_{C-P}$ = 2 Hz), 130.29 (d, $^3J_{C-P}$ = 17 Hz), 131.42 (d, $^3J_{C-P}$ = 2 Hz), 142.80 (d, $^1J_{C-P}$ = 6 Hz). ^{31}P NMR (162 MHz, acetone-d_6): δ (ppm) −119.76. IR: ν (cm^{-1}) = 1647 (s, CH=CH_2), 1081 (vs, ClO_4^-). Anal. Calcd (%) for $C_{30}H_{30}Cl_2N_{12}O_8P_2Zn\cdot 2H_2O$: C, 39.13; H, 3.72; N, 18.25. Found: C, 39.06; H, 3.82; N, 18.70.

(c) [Cu(1)$_2$](ClO$_4$)$_2$ (3). $[Cu(OH_2)_6](ClO_4)_2$ (74.1 mg, 200 μmol) was added to a solution of ligand **1** (67.3 mg, 200 μmol) in methanol (10.0 mL). A blue precipitate was formed immediately. After 24 h, it was isolated, washed with methanol, and dried in a vacuum (yield: 152 mg, 84%). IR: ν (cm^{-1}) = 1640 (s, CH=CH_2), 1075 (vs, ClO_4^-). Anal. Calcd (%) for $C_{30}H_{30}Cl_2CuN_{12}O_8P_2\cdot 1.5H_2O$: C, 39.59; H, 3.65; N, 18.47. Found: C, 39.20; H, 3.72; N, 18.93.

(d) [Mo(η^3-C$_3$H$_5$)(CO)$_2$(1)](BF$_4$) (4). $AgBF_4$ (479 mg, 2.46 mmol) was added to a stirred suspension of [Mo(η^3-C_3H_5)Cl(CH_3CN)$_2$(CO)$_2$] (631 mg, 2.46 mmol) in acetonitrile (60 mL). After 15 min the AgCl precipitate was removed by filtration and ligand **1** (827 mg, 2.46 mmol) was added. After 30 min the solvent volume was reduced to 5 mL, filtered, and poured into diethyl ether (100 mL). The yellow precipitate was isolated, washed several times with diethyl ether, and dried in a vacuum (yield: 845 mg, 55%). Crystals were obtained by slow diffusion of diethyl ether into a CH_3CN solution of **4**. ^{1}H NMR (400 MHz, CD_3CN): δ (ppm) 1.71 (d, ^2J = 12 Hz, 2 H, H_{allyl}), 3.72 (s, ^2J = 8 Hz, 2 H, H_{allyl}), 3.84−3.92 (m, 1 H, H_{allyl}), 5.23−5.29 (m, 3 H, CH=CH_2), 5.47−5.64 (m, 3 H, CH=CH_2), 7.40 (br, 3 H, CH=CH_2), 7.61 (s, 2 H, H_{Im}), 7.65 (s, 2 H, H_{Im}), 7.71 (s, 1 H, H_{Im}), 8.35 (s, 1 H, H_{Im}). ^{13}C NMR (101 MHz, CD_3CN): δ (ppm) 60.52, 75.72, 108.02, 108.66, 116.95, 120.86, 130.31 (d, $^3J_{C-P}$ = 17 Hz), 133.85, 138.30, 227.76 (s, CO). ^{31}P NMR (162 MHz, CD_3CN): δ (ppm) −112.28. IR: ν (cm^{-1}) = 1943 (vs, CO), 1855 (vs, CO), 1646 (s, CH=CH_2), 1051 (vs, BF_4^-). Anal. Calcd (%) for $C_{20}H_{20}BF_4MoN_6O_2P\cdot 0.5CH_3CN\cdot H_2O$: C, 40.12; H, 3.77; N, 14.48. Found: C, 39.90; H, 3.40; N, 14.72.

(e) [Mo(η^3-C$_4$H$_7$)(CO)$_2$(1)](TsO) (5). AgOTs (681 mg, 2.44 mmol) was added to a stirred suspension of [Mo(η^3-C_4H_7)Cl(CH_3CN)$_2$(CO)$_2$] (660 mg, 2.44 mmol) in acetonitrile (50 mL). After 15 min the AgCl precipitate was removed by filtration and ligand **1** (821 mg, 2.44 mmol) was added. After 30 min the solvent volume was reduced to 5 mL, filtered, and poured into diethyl ether (100 mL). The yellow precipitate was isolated, washed several times with diethyl ether, and dried in a vacuum (yield: 980 mg, 55%). Crystals were obtained by slow diffusion of diethyl ether into a CH_3CN solution of **5**. ^{1}H NMR (400 MHz, CD_3CN): δ (ppm) 1.51 (s, 2 H, H_{allyl}), 1.54 (s, 3 H, TsO−), 2.32 (s, 3 H, CH_3), 3.63 (s, 2 H, H_{allyl}), 5.07 (d, ^3J = 8 Hz, 1 H, CH=CH_2), 5.24 (d, ^3J = 8 Hz, 2 H, CH=CH_2), 5.48 (d, ^3J = 16 Hz, 1 H, CH=CH_2), 5.58 (d, ^3J = 16 Hz, 2 H, CH=CH_2), 7.14 (d, ^3J = 8 Hz, 2 H, TsO−), 7.21 (s, 2 H, H_{Im}), 7.37 (br, 2 H, H_{Im}), 7.50 (dd, ^3J_E = 16 Hz, ^3J_Z = 8 Hz, 3 H, CH=CH_2), 7.59 (d, ^3J = 8 Hz, 2 H, TsO−), 7.64−7.68 (m, 2 H, H_{Im}). ^{13}C NMR (101 MHz, CD_3CN): δ (ppm) 18.29 (CH_3−TsO), 21.28 (C_{allyl}), 61.18 (C_{allyl}), 83.83 (C_{allyl}), 107.08, 108.23 (br), 117.37, 120.97, 120.97, 121.54, 126.71, 129.25, 130.14, 130.43 (d, $^3J_{C-P}$ = 17 Hz), 133.24 (d, $^1J_{C-P}$ = 6 Hz), 139.46, 146.85, 227.24 (CO). ^{31}P NMR (162 MHz, CD_3CN): δ (ppm) −111.93. IR: ν (cm^{-1}) = 1935 (vs, CO), 1836 (vs, CO), 1643 (s, CH=CH_2). Anal. Calcd (%) for $C_{28}H_{31}MoN_6O_5PS\cdot 0.5CH_3CN\cdot H_2O$: C, 47.77; H, 4.77; N, 12.49. Found: C, 47.24; H, 4.29; N, 12.86.

(f) Polymer P1−Cu. Ligand **1** (2.00 g, 5.95 mmol) and AIBN (122 mg, 743 μmol) were dissolved in MeOH (14.0 mL) and heated for 24 h at 65 °C in a closed screw cap vial. The pale yellow, insoluble polymer was isolated, dried in a vacuum, ground in a mortar, and washed with MeOH (5 × 40 mL). After drying in a vacuum, a pale yellow powder **P1** was obtained (yield: 1.76 g, 88%). Metalation was achieved by mixing a solution of anhydrous $CuCl_2$ in MeOH (40 mL, 0.5 M) with the polymer (1.37 g) for 20 min. The resulting dark green polymer **P1−Cu** was washed with MeOH until the reaction with dithiooxamide was negative (5 × 80 mL) and dried in a vacuum. IR: ν (cm^{-1}) = 1642 (w, CH=CH_2). ICP-OES: 126 mg of Cu/g of polymer.

(g) Polymer P2−Cu. Ligand **1** (332 mg, 0.987 mmol), EGDMA (710 mg, 3.58 mmol), and AIBN (100 mg, 609 μmol) were dissolved in MeOH (10.0 mL) and heated for 24 h at 65 °C in a closed screw cap vial. The pale yellow, insoluble polymer was isolated, dried in a vacuum, ground in a mortar, and washed with MeOH (5 × 40 mL). After drying in a vacuum, a pale yellow powder **P2** was obtained (yield: 905 mg, 87%). Metalation was achieved by mixing a solution of anhydrous $CuCl_2$ in MeOH (40 mL, 0.5 M) with the polymer **P2** for 20 min. The resulting dark green polymer **P2−Cu** was washed with MeOH until the reaction with dithiooxamide was negative (6 × 40 mL) and dried in a vacuum. IR: ν (cm^{-1}) = 1722 (vs, EGDMA), 1646 (w, CH=CH_2). ICP-OES: 46 mg of Cu/g of polymer.

(h) Polymer P3−Mo. Complex **5** (755 mg, 1.04 mmol), EGDMA (710 mg, 3.58 mmol), and AIBN (100 mg, 609 μmol) were dissolved in acetonitrile (34 mL) and heated for 5 h at 65 °C and then 19 h at 70 °C in a closed screw cap vial. The yellow, insoluble polymeric gel was isolated, dried in a vacuum, ground in a mortar, and washed with acetonitrile (4 × 100 mL). After drying in a vacuum, a yellow powder was obtained (yield: 1.19 g, 81%). IR: ν (cm^{-1}) = 1939 (s, CO), 1847 (s, CO), 1720 (vs, EGDMA), 1644 (w, CH=CH_2). ICP-OES: 26 mg of Mo/g of polymer.

(i) Polymer P3. The polymer **P3−Mo** (999 mg) was suspended in HNO_3 (25 mL, 65%) for 30 min at room temperature. Subsequently, it was washed with water (25 mL), with $NaOH_{aq}$ (2 × 40 mL, 1 M), and with H_2O/MeOH 1:1 (4 × 40 mL). Finally **P3** was washed with MeOH (40 mL) and acetone (40 mL) and dried in a vacuum (yield: 723 mg). IR: ν (cm^{-1}) = 1718 (vs, EGDMA), 1652 (w, CH=CH_2).

(j) Polymer P3−Cu. Metalation was achieved by mixing a solution of anhydrous $CuCl_2$ in MeOH (40 mL, 0.5 M) with the polymer (614 mg) for 20 min. The resulting dark green polymer **P3−Cu** was washed with MeOH until the reaction with dithiooxamide was negative (6 × 40 mL) and then it was dried in a vacuum (yield: 647 mg). IR: ν (cm^{-1}) = 1718 (vs, EGDMA), 1652 (w, CH═CH_2). ICP-OES: 30 mg of Cu/g of polymer, 7.0 mg of Mo/g of polymer.

Kinetic Investigations. The hydrolysis of BNPP and NPP by the polymers **P1−Cu**, **P2−Cu**, and **P3−Cu** was carried out in 70 mM buffered aqueous solution (MES, HEPES, HEPPSO, and CHES). After an incubation time of 30 min, the reactions were initiated by addition of a freshly prepared stock solution of the substrate (final concentration: 5.0 mM). After a given time, the reaction tubes were centrifuged for 1 min and the absorbance A of the clear supernatant was determined by UV/Vis at λ = 400 nm. Pseudo-first-order rate constants were obtained by linear least-squares regression (R > 0.998) from a plot of $-\ln(1 - A/A_{max})$ versus time. For the determination of initial rates, the concentration of the hydrolysis product, *p*-nitrophenolate anion, was calculated from the absorbance A and the extinction coefficient (ϵ = 18700 M^{-1} cm^{-1}) by correction for the degree of ionization of *p*-nitrophenol (pK_a 7.15). Initial rates were obtained by linear least-squares regression (R > 0.998) from a plot of concentration of hydrolysis product against time. Reactions were monitored at 25 °C to less than 5% conversion of substrate to product. The buffers were HEPES (pH 7.0), HEPPSO (pH 7.5−8.0), and CHES (pH 8.5−9.0) and pH remained constant within the error range after the experiment. Spontaneous hydrolysis was minimal across the pH range studied (6.0−9.0). No correction of background hydrolysis was effected as it can be considered as negligible.

For the determination of the Michaelis−Menten kinetics, plots of initial velocities of the catalyzed hydrolysis versus substrate concentration were measured. Initial reaction rates were monitored at constant concentration of the active sites and varying substrate concentrations. Michaelis−Menten parameters were obtained by linear least-squares regression (R > 0.999) from a Lineweaver−Burk plot.

Potentiometric Titration. Polymer **P3−Cu** (22.1 mg) was suspended in deionized water (3.0 mL) and was titrated with $CsOH_{aq}$ (0.1 M).

Elemental Analysis of Polymers (ICP-OES). A suspension of the respective polymer (10−25 mg) was heated in concentrated sulfuric acid (2 mL) at 140 °C for 2 h in a volumetric flask (25.0 mL). Hydrogen peroxide (30%, 0.5−1 mL) was subsequently added, and the colorless solution was heated for 12 h at 140 °C. The resulting clear solution was diluted to 25.0 mL with nitric acid (2%, aqueous) and analyzed by ICP-OES. Every Mo and Cu analysis was done in duplicates and the error was less than 1.5%.

Swelling Ratio of the Polymers. The dried polymers were immersed in NMR tubes with 4 mL of deionized water at 25 °C until swelling equilibrium was attained after 48 h. The volume increase was measured with a ruler. The swelling ratio (Q) based on V_d (dry volume) and V_w (wet volume) was calculated from the following equation: Swelling ratio $Q = V_w/V_d$. All measurements were performed in duplicates and the error was less than 3.0%.

Crystallographic Investigations. The crystal data and structure refinement for compounds **1**, **2**, **4**, and **5** are listed in Tables 2 and 3 whereas the relevant geometrical parameters are shown in the figure captions (see Figures 1, 2, 3, and 4). Data collection has been performed at 140(2) K using Mo Kα radiation on different equipment: a marresearch mar345 IPDS (**1** and **2**) or a four-circle kappa goniometer with an Oxford Diffraction KM4 Sapphire CCD (**4** and **5**). Cell refinement and data reduction has been carried out with the aid of CrysAlis RED 1.7.1 β release.[32] A semiempirical absorption correction (MULTI-SCAN)[33] has been applied to all data sets. All structures were refined using the full-matrix least-squares

Table 2. Crystallographic Data for the Compounds **1** and **2**

	1·0.5C_6H_6	**2**·2CH_3OH·0.5H_2O
empirical formula	$C_{18}H_{18}N_6P$	$C_{32}H_{39}C_{l2}N_{12}O_{10.5}P_3Zn$
mol wt [g mol^{-1}]	349.35	957.96
cryst size	0.12 × 0.10 × 0.08	0.18 × 0.15 × 0.15
cryst syst	triclinic	orthorhombic
space group	$P\bar{1}$	*Pccn*
a [Å]	7.9426(14)	14.908(5)
b [Å]	9.506(4)	15.273(5)
c [Å]	11.930(5)	18.302(3)
α [deg]	89.12(4)	90
β [deg]	80.58(2)	90
γ [deg]	77.85(2)	90
V [$Å^3$]	868.6(6)	4167(2)
Z	2	4
d [g cm^{-3}]	1.336	1.527
T [K]	140(2)	140(2)
abs coeff [mm^{-1}]	0.172	0.864
Θ range [deg]	3.07−25.03	2.93−25.03
index ranges	−8 → 8	−17 → 17
	−11 → 11	−18 → 18
	−14 → 14	−21 → 21
reflns collected	5648	25415
indep reflns	2889 [R_{int} = 0.0300]	3681 [R_{int} = 0.0611]
abs correction	semiempirical	semiempirical
max and min transm	1.0318 and 0.9107	0.9151 and 0.8480
data/restraints/params	2889/0/227	3681/2/274
GOF on F^2	1.097	1.074
final R indices [$I > 2\sigma(I)$]	R1 = 0.0497	R1 = 0.0503
	wR2 = 0.1355	wR2 = 0.1319
R indices (all data)	R1 = 0.0581	R1 = 0.0780
	wR2 = 0.1492	wR2 = 0.1474
largest diff peak/hole [e $Å^{-3}$]	0.358/−0.380	0.344/−0.409

Table 3. Crystallographic Data for the Compounds **4** and **5**

	4	**5**·0.5C_4H_6O
empirical formula	$C_{20}H_{20}BF_4MoN_6O_2P$	$C_{30}H_{34}MoN_6O_{5.5}PS$
mol wt [g mol^{-1}]	590.14	725.60
cryst size	0.16 × 0.14 × 0.11	0.18 × 0.12 × 0.08
cryst syst	monoclinic	triclinic
Space group	$P21/n$	$P\bar{1}$
a [Å]	10.7335(4)	8.2044(13)
b [Å]	16.0022(10)	11.7633(17)
c [Å]	13.6290(9)	18.087(3)
α [deg]	90	79.757(12)
β [deg]	94.322(5)	88.807(13)
γ [deg]	90	70.442(14)
V [$Å^3$]	2334.3(2)	1617.3(4)
Z	4	2
d [g cm^{-3}]	1.679	1.490
T [K]	140(2)	140(2)
abs coeff [mm^{-1}]	0.694	0.569
range [deg]	2.95-25.03	3.21-25.03
index ranges	−11 → 11	−8 → 9
	−19 → 19	−13 → 13
	−16 → 16	−21 → 21
reflns collected	13364	9827
indep reflns	3964 [R_{int} = 0.0306]	4990 [R_{int} = 0.0884]
abs correction	semiempirical	semiempirical
max and min transm	0.9542 and 0.8489	1.0947 and 0.7925
data/restraints/params	3964/0/317	4990/0/407
GOF on F^2	1.055	0.879
final R indices [$I > 2\sigma(I)$]	R1 = 0.0371	R1 = 0.0602
	wR2 = 0.0943	wR2 = 0.1192
R indices (all data)	R1 = 0.0470	R1 = 0.1218
	wR2 = 0.0983	wR2 = 0.1366
largest diff peak/hole [e $Å^{-3}$]	1.413/−0.712	0.974/−1.083

on F^2 with all non-H atoms anisotropically defined. The hydrogen atoms were placed in calculated positions using the "riding model". Some antibumping restraints have been applied in the case of compound **2**. Structure refinement and geometrical calculations were carried out on all structures with SHELXTL 5.1.[34]

(32) Oxford Diffraction Ltd.: Abingdon, Oxfordshire, U.K., 2005.
(33) Blessing, R. H. *Acta Crystallogr., Sect. A* **1995**, *51*, 33−38.
(34) Sheldrick, G. M. *SHELXTL*; University of Göttingen: Göttingen, Germany 1997; BrukerAXS, Inc.: Madison, WI, 1997.

Acknowledgment. This work was supported by the Swiss National Science Foundation and the DFG. We thank Meriem Benmelouka for measuring the EPR spectra.

Supporting Information Available: X-ray crystallographic data in CIF format for ligand 1 and complexes **2**, **4**, and **5**. This material is available free of charge via the Internet at http://pubs.acs.org.

IC0504588